Universities of Leeds, Sheffield and York
http://eprints.whiterose.ac.uk/

Published paper
Batterbee, D.C. and Sims, N.D. (2005) *Vibration isolation with smart fluid dampers: a benchmarking study.* Smart Structures and Systems, 1 (3). pp. 235-256.

Vibration isolation with smart fluid dampers: a benchmarking study

D C Batterbee and N D Sims[*]

Department of Mechanical Engineering, The University of Sheffield,

Sheffield, S1 3JD, UK.

ABSTRACT

The non-linear behaviour of electrorheological (ER) and magnetorheological (MR) dampers makes it difficult to design effective control strategies, and as a consequence a wide range of control systems have been proposed in the literature. These previous studies have not always compared the performance to equivalent passive systems, alternative control designs, or idealised active systems. As a result it is often impossible to compare the performance of different smart damper control strategies.

This article provides some insight into the relative performance of two MR damper control strategies: on/off control and feedback linearisation. The performance of both strategies is benchmarked against ideal passive, semi-active and fully active damping. The study relies upon a previously developed model of an MR damper, which in this work is validated experimentally under closed-loop conditions with a broadband mechanical excitation. Two vibration isolation case studies are investigated: a single-degree-of-freedom mass-isolator, and a two-degree-of-freedom system that represents a vehicle suspension system. In both cases, a variety of broadband mechanical excitations are used and the results analysed in the frequency domain. It is shown that although on/off control is more straightforward to implement, its performance is worse than the feedback linearisation strategy, and can be extremely sensitive to the excitation conditions.

---

[*] Corresponding author. Email: n.sims@sheffield.ac.uk; Tel: +44 114 2227724.

1   INTRODUCTION

There is substantial interest in the use of magnetorheological (MR) and electrorheological (ER) fluids to provide semi-active damping in vibration control. In these devices, the level of damping can be altered through the application of an electric (for ER) or magnetic (for MR) field. Such dampers have the potential to outperform their passive counterparts and this has recently led to commercial success (Jolly *et al.* 1998). However, despite this success, a wide variety of control strategies are in use (either experimentally or commercially) and as yet, there is no consensus on how best to perform automatic control.

A key reason for this is the inherent non-linear behaviour of smart fluid devices, which makes the goal of tracking a prescribed force demand a challenging task. Consequently, investigators have focused on the development of relatively complex semi-active controllers, in an attempt to fully exploit their potential within automatic control systems. For example, Lyapunov stability theory and clipped optimal control strategies have been implemented in structural control with some success (Dyke *et al.* 1998; Jansen and Dyke 2000; Yi *et al.* 2001) and have been shown to compare well with equivalent ideal semi-active and fully active systems (Yoshida and Dyke 2004). Neural networks have also been investigated for both structural (Xu *et al.* 2003) and automotive (Guo *et al.* 2004) applications incorporating magnetorheological dampers, as well as fuzzy control schemes (Atray and Roschke 2004). Furthermore, investigators have implemented sliding mode control, for example, in automotive (Lam and Liao 2003) and aerospace (Choi and Wereley 2003) applications.

With many of these control strategies, investigators have simplified the force tracking strategy by using on/off or bang-bang methods. Examples include the optimal control of structures (Jansen and Dyke 2000; Yi *et al.* 2001; Yoshida and Dyke 2004) and skyhook control of vehicle suspensions (Simon and Ahmadian 2001), where the smart damper current is switched

to a pre-determined level when a dissipative force is required within the controllable range of the device. Alternatively, approximate linear relationships between the control current and the maximum damping force have been investigated (Yoshida and Dyke 2004). Research at the University of Sheffield has pursued an alternative approach to controller design, which first linearises the damper's behaviour using force feedback (Sims *et al.* 1999c; 2000). This feedback linearisation permits accurate set-point force tracking within the control limits imposed by the fluid properties and device geometry, thus enabling various control algorithms to be implemented more effectively. Furthermore, as the present study will show, feedback linearisation desensitises the controlled system performance to parameter uncertainties such as the disturbance input and fluid properties.

In a previous numerical study based upon an ER damper (Sims *et al.* 2001), this control approach was shown to be effective for a single-degree-of-freedom (SDOF) mass-isolator with sinusoidal excitation. A later article (Sims and Stanway 2003) extended this work to investigate a two-degree-of-freedom (2DOF) structure representing a vehicle suspension system. Although a broadband mechanical excitation was used, the model had not been formally validated under such circumstances, and the excitation conditions were not representative of actual roadways. The present study aims to overcome these issues raised by the earlier work, and to illustrate the performance of the feedback linearisation strategy in comparison with on/off control schemes. Furthermore the MR systems are benchmarked against idealised passive, semi-active and fully active dampers. The study is based upon a previously developed model of an MR damper and new experimental results are used to validate this model under closed-loop conditions with a broadband mechanical excitation. Two numerical case studies are investigated: an SDOF mass-isolator with a variety of broadband excitation signals, and a 2DOF system (representing a vehicle suspension) excited by realistic road profiles (Cebon and Newland 1984; Robson 1979).

In both case studies, feedback linearisation is demonstrated by implementing skyhook based control laws. This approach has received much attention in vibration control when Karnopp (1974) originally demonstrated that it was an optimal control strategy for an SDOF mass isolator. The approach is illustrated in Figure 1 where, by applying an actuation force that is directly proportional to the absolute velocity of the vibrating mass, both the low *and* high frequency response of the system can be significantly enhanced. This normally requires a fully active actuator, but semi-active devices have been shown to perform nearly as well (Karnopp *et al.* 1974).

The paper is organised as follows. After describing the modelling strategy for the MR damper, the theory of feedback linearisation is summarised and experimental results are compared to model predictions. Next, the SDOF control system models are described before presenting the corresponding results, and the 2DOF investigation is then presented in a similar manner. Finally some general issues are discussed and conclusions are drawn.

2   MR DAMPER MODEL

In earlier work (Sims and Wereley 2003; Sims *et al.* 2004) a general modelling approach was described that can be applied to a variety of smart fluid devices, and enables a model updating or system identification procedure to be performed so that the model can be adjusted in line with observed behaviour. In the present study, the model developed by Sims *et al.* (2004) will be used, and this model is summarised here for the sake of completeness.

The model is based on Lord Corporation's RD-1005-3 MR damper (Lord Corporation 2004) and a schematic drawing of this device is shown in Figure 2(a). This is a flow mode (Sims *et al.* 1999a) device where movement of the piston rod forces fluid through an annular orifice. An accumulator is also incorporated to accommodate for the change in the working volume caused by the presence of the piston rod. This introduces an element of stiffness to the

damper response, however this was found to be insignificant when compared to the suspension stiffness terms in the SDOF and 2DOF models. Consequently, the effect of the accumulator has been neglected in the development of the MR damper model.

The form of the model is a bi-viscous damper in series with a mass and a linear spring, as shown in Figure 2(b), and can be strongly linked to the constitutive behaviour of the device. For example, the valve flow (which is assumed to be quasi-steady) is represented by the non-linear function χ and is a function of the quasi-steady velocity $\dot{x}_1$ and the control signal I to the smart damper. The spring element of stiffness k is incorporated to account for fluid compressibility and the lumped mass m_1 represents fluid inertia. The co-ordinate x_2 corresponds to the displacement of the damper piston.

This physical significance means that parameters can initially be chosen based on constitutive relationships using fluid properties such as bulk modulus, viscosity and yield stress (Sims *et al.* 1999b). However, in practice, fluid properties may vary between devices, for example due to environmental effects or manufacturing tolerances. Consequently, a model updating procedure is desirable so that the model accurately predicts observed behaviour. This procedure has been adopted to form an accurate model of the commercial MR damper used in this study. A description of this model updating procedure is detailed by Sims *et al*. (2004).

Figure 3 compares a typical set of predictions from the updated model with the corresponding test data for a range of sinusoidal excitation conditions. The model results agree very well with observed behaviour. The previous study (Sims *et al.* 2004) also validated the model under non-sinusoidal test conditions, making the model an appropriate tool for the present investigation. Furthermore it was demonstrated that the dynamics of the electro-magnetic circuit and smart fluid rheology could be modelled using a first order lag term, where a time

constant between 3-5ms was shown to be accurate. Throughout this study, a 3ms device time constant has been used as part of the controlled MR systems.

3   FEEDBACK LINEARISATION

The non-linear behaviour of smart fluid dampers makes the objective of achieving a desired force very difficult. Work by the authors and their colleagues has developed one solution to this problem using feedback linearisation, which is briefly summarised below.

The control strategy is shown in block diagram form in Figure 4(a). Here, feedback control is being used to implement a semi-active force generator. Through appropriate selection of the feedforward gain G, and the feedback gain B, it can be shown how the actual damping force F becomes equal to the desired set-point damping force F_d (Sims *et al.* 1999c). If the set-point force is proportional to the piston velocity then the force-velocity response is linearised. For the present study, the values of G and B were determined through extensive experimental testing leading to G = 0.0015 and B = 0.6.

Figure 4(b) shows schematically how feedback linearisation can be integrated within a vibrating structure such as a mass-isolator or vehicle suspension. Here, the linearised damper is able to track a force demand derived from a separate controller, for example a skyhook or optimal controller. However, the desired force will only be met if it lies within the control limits imposed by the device geometry and MR fluid properties. This is better described with the help of Figure 5, which illustrates the control envelope of the MR damper. If the desired force lies within this envelope, then feedback linearisation can accurately achieve that force. However if an energy input is required i.e. the desired force lies within quadrants 2 and 4, or if a dissipative force level (within quadrants 1 and 3) is lower than that governed by the base viscosity of the fluid (I=0A), then this force cannot be achieved. In this scenario, the MR

damper will remain in its 'off' state to minimise the energy dissipated. Alternatively, if the desired force is a dissipative one and exceeds the upper boundary of the control envelope (I=2A), then the damper current will saturate at its maximum level to maximise the energy dissipated.

3.1 Validation

In previous work, the proposed linearisation technique has been shown to be effective for an ER damper under sinusoidal mechanical excitation (Sims *et al.* 1999c; 2000). However, the present study was based upon a model of a commercially available MR damper and the simulated mechanical excitation was non-sinusoidal. Consequently it was necessary to validate this model under closed loop conditions with a broadband mechanical excitation.

To achieve this, the damper was mounted in a servohydraulic test machine operating in its displacement control mode with a nonsinusoidal command signal. This was generated by filtering a white noise signal to reduce its high frequency content (i.e. above 25Hz) to within the capabilities of the test machine. Meanwhile, a real-time digital signal processing system (xPC Target 2002) was used to implement the feedback linearisation strategy. With reference to Figure 4(a), the set-point F_d was made proportional to the mechanical excitation velocity:

$$F_d = Dv \tag{1}$$

Here, v is the damper excitation velocity (equivalent to $\dot{x}_2$ for the model shown in Figure 2) and D is a controller set-point gain. The feedback strategy should result in viscous damping behaviour with an effective damping rate equal in value to the controller gain D.

Figure 6 shows a sample of the input displacement signal and Figure 7(a) shows the resulting force-velocity responses for a range of set-point gains between D = 2kNs/m and D = 20kNs/m. Shown superimposed are straight lines of slope D, which represent the idealised

7

responses. Very good linearisation is demonstrated for values of D between 2 and 10kNs/m thus validating the controller's behaviour under broadband excitation. For the set-point $D =$ 20kNs/m, the control limits of the MR damper can be observed. For example, the force beyond $\pm$ 0.08m/s is less than the ideal viscous force, resulting in a non-linear response.

To validate the model under closed loop conditions, Figure 7(b) shows the simulated linearised responses under identical excitation and controller conditions as for the experiment. Again, highly linear characteristics can be observed with the actual responses closely matching the ideal responses. Moreover, the simulated results correlate very well with the experiment and the onset of saturation in the response (D=20kNs/m) is predicted accurately.

4   SDOF STUDY

Having demonstrated the experimental and simulated performance of the feedback linearisation strategy under broadband excitation, the approach will now be used as part of a simulated mass-isolator vibration problem. The performance will be benchmarked against a range of idealised systems and an on/off control strategy. For each system, the input excitations and, where applicable, the MR damper model were identical in order to permit a direct comparison between them. The mass-isolator and damper control configurations are now described, before presenting the simulated results.

4.1   Mass-isolator configurations

The basic parameters for the mass-isolator were chosen to give a system natural frequency of 5Hz and a damping ratio of 0.1 when the MR damper was in its 'off' state. This frequency is well within the range of frequencies validated experimentally and resulted in a mass M of 115kg and a spring stiffness K_{iso} of 113.5kN/m. Three different broadband displacement inputs were investigated for each system. The first input was generated with a constant

8

velocity amplitude (i.e. white noise) over the frequency range 0-100Hz. The second and third inputs were generated by passing this signal through a finite impulse response filter, designed with a least squares method to produce cut off frequencies at 25Hz and 10Hz respectively.

Five damper configurations were investigated and these are described below.

- **Passive system**

Previous studies have not always compared the performance of MR systems to equivalent passive systems. For example, investigators commonly use the MR damper in its 'on' or 'off' state to represent a passive suspension (Lam and Liao 2003). In the 'off' state, the damping is likely to be less than that of a well-damped passive device, whereas in the 'on' state the damping will be higher than a well-damped passive device. A more realistic passive benchmark was used in the present study where the damping force was generated by a viscous damper with damping coefficient C_p as shown in Figure 8(a). C_p was varied to optimise the passive system response to enable a true performance comparison with the MR systems.

- **MR linearised skyhook control**

With reference to Figure 8(b), the set-point force was given by:

$$F_d = D_{MR}\dot{x}_m \qquad (2)$$

The controller subsystem of Figure 8(b) corresponds to that shown in Figure 4(a). As discussed in section 3, the MR damper may not achieve the set-point force, particularly when the set-point lies outside the control limits of the damper (shown in Figure 5).

- **On/off skyhook control**

In semi-active vibration control, on/off skyhook control strategies are commonly investigated (Cebon *et al.* 1996; Simon and Ahmadian 2001). The strategy involves switching the input

current to a predetermined and constant level when the force required by the skyhook control law is a dissipative one:

$$I = I_{max}: \qquad \dot{x}_m(\dot{x}_m - \dot{x}_b) \geq 0 \; - \; \text{Energy dissipation required} \tag{3}$$

$$I = 0: \qquad \dot{x}_m(\dot{x}_m - \dot{x}_b) < 0 \; - \; \text{Energy input required} \tag{4}$$

The controller gain I_{max} dictates the current applied in the 'damper on' condition. Since no force feedback is required, the need to measure or estimate the damping force is eliminated. On/off skyhook control therefore represents a major simplification over the linearised skyhook controller. However, the performance may suffer, and by studying the behaviour of the two controllers under identical circumstances, a true comparison can be made.

- **Fully active skyhook control**

In this system, the desired skyhook force was assumed to be produced by an ideal force actuator capable of instantaneously supplying and dissipating energy. This represents the ideal skyhook system and will act as an upper boundary of performance for the MR damper systems. The fully active system is shown in Figure 8(c), where the force F is given by:

$$F = D_{IS}\dot{x}_m \tag{5}$$

- **Ideal semi-active skyhook control**

In this system the desired skyhook force is achieved only if the force is a dissipative one, otherwise zero damping force is transmitted:

$$F = D_{SAS}\dot{x}_m: \qquad \dot{x}_m(\dot{x}_m - \dot{x}_b) \geq 0 \tag{6}$$

$$F = 0: \qquad \dot{x}_m(\dot{x}_m - \dot{x}_b) < 0 \tag{7}$$

This will act as a more realistic upper performance boundary for the MR based systems.

4.2 Results

First, the MR linearised skyhook system is compared with the fully active skyhook system. Figure 9(a) shows the transmissibility curves, obtained using Welch's method (1967), for the displacement input filtered to 25Hz. The passive response for C_p = 2kNs/m is also shown since, of all the passive damping rates for this particular input, it had the lowest root-mean-square (RMS) acceleration, which is an important performance indicator. As expected, the fully active system improves both the low and high frequency response with increasing controller gain D_{IS}. This is superior to the MR system where a slight degradation in the high frequency response is observed with increased controller gain D_{MR}. Nonetheless, there is a significant improvement over the passive system.

Figure 9(b) compares the transmissibility curves, again for the displacement input filtered to 25Hz, between the linearised MR skyhook system and the idealised semi-active skyhook system, which represents a more realistic performance benchmark. For skyhook gains of 3kNs/m, it can be seen how the frequency response of the MR system around the natural frequency is better than the ideal semi-active system, but worse at higher frequencies. For skyhook gains of 6kNs/m, the semi-active system is superior throughout the frequency range.

Figure 9(c) compares the transmissibility curves between the linearised MR skyhook and the on/off MR skyhook systems. Much like a passive system, there is a clear compromise between the low and high frequency performance of the on/off system with increasing controller gain I_{max}. For example, the low frequency response is superior to the MR system for large gains, but this is at the expense of a poorer high frequency response compared to both MR and passive systems.

It is difficult to get a clear indication of the relative performance between the above systems using transmissibility plots alone. For example, a trade-off has been demonstrated between

the low and high frequency responses when the controller gain is increased and thus it becomes difficult to determine an optimum value. Direct comparison is made more straightforward when a conflict diagram is used. This is where the RMS value of one performance indicator is plotted against that for another, as a controller gain is varied. This not only helps to optimise the control systems but also gives clarity on the inevitable trade-offs between the performance indicators themselves. Suitable performance indicators are the RMS acceleration, which represents the severity of the vibration of the mass, and the RMS working space, which is a common design constraint. The conflict diagram has also been used as a means to compare the three different displacement inputs. Figure 10 presents the conflict diagrams for each of the input excitations.

In case of the input signals filtered to 10Hz (Figure 10(a)) and 25Hz (Figure 10(b)), feedback linearisation is seen to enhance RMS acceleration compared to the on/off control strategy. For the unfiltered input signal containing frequencies up to 100Hz (Figure 10(c)), there appears to be no significant advantage gained by implementing feedback linearisation, where RMS acceleration levels are similar to the on/off system.

With regards to the benchmark systems, Figure 10 demonstrates how the ideal semi-active and fully active skyhook systems are superior in terms of acceleration, but this is at the expense of larger working spaces. Furthermore, the performance benefits of a fully active system are substantially better than the ideal semi-active system if larger working spaces can be tolerated.

To better illustrate the relative performance between systems, optimum controller gains (i.e. D_{MR}, D_{IS}, D_{SAS}, I_{max} and C_p) were chosen for the input signal filtered to 10Hz such that RMS acceleration was minimised. These gains, which are shown in Table 1, were then maintained for all three excitation conditions and the resulting performance is indicated on Figure 10.

Figure 11 then compares the percentage performance improvements of the controlled systems over the optimised passive system at the chosen operating points. For the signal filtered to 10Hz, this resulted in a 25% reduction in RMS acceleration for the linearised system compared to a 15% reduction for the on/off system. The optimised on/off system performs quite well, but when analysing the position of the operating points on Figures 10(b) and 10(c), a key advantage of feedback linearisation becomes apparent. From Figure 11, it can be observed how RMS acceleration for the linearised system remains consistently low regardless of the input conditions. By comparing Figures 10(a) and 10(b), this is because the shape of the conflict curve, and thus the optimum controller gain D_{MR}, remains unchanged. On the other hand, the on/off system is very sensitive to the input conditions and RMS acceleration levels are degraded as frequency content increases. This occurs because of the change in shape of the conflict curve between Figures 10(a) and 10(b), which also explains the improved working space levels. Therefore the 'straightforward' on/off system may in fact need a rather more complex control strategy to alter the controller gain according to input excitation. This would be necessary to ensure that its implementation is justifiable against its passive counterpart.

For the linearised system subject to the unfiltered signal (Figure 10(c)), there is a change in shape of the conflict curve compared to Figures 10(a) and 10(b). However performance does not suffer due to its shallow gradient. It should be noted that the accuracy of the results presented in Figure 10(c) and Figure 11(c) is less certain, because the MR damper model does not take into account high frequency behaviour, and has not been validated above 25Hz. At high frequencies, seal friction effects and device joints may have an important role. Also, the attenuation of high frequency vibrations is likely to be outside the duty of the isolator, due to the compliance of the mechanical connections and bushings.

Finally, to illustrate performance of the benchmark systems, Figure 11(a) demonstrates a 64% improvement in acceleration for the fully active system compared to 36% for the ideal semi-active system. This is clearly superior to the MR systems, however the corresponding working spaces are 58% and 18% worse than the passive system respectively. This is a consistent result across the range of excitation conditions.

5   2DOF STUDY

The results presented so far have demonstrated the relative performance of two MR damper control strategies, compared to ideal passive, semi-active and fully active dampers. In this section, the analysis is repeated using a two degree of freedom system that is representative of a vehicle suspension problem. As before, the same input excitations and MR damper model (where applicable) were used for each control system in order to permit a direct comparison between the control strategies.

It should be mentioned that the MR damper under investigation was not specifically designed for use in a vehicle suspension. However, the intention here is not to fine-tune the actual device for a specific vehicle but rather to demonstrate the performance potential of linearising an MR damper to implement semi-active vehicle control strategies. For this purpose, a simplified vehicle model serves as a useful case study. The vehicle model is first described before presenting the simulated results.

5.1   Quarter car model

In the design of suspension for passenger vehicles, it is desirable to achieve low levels of car body acceleration, thus ensuring passenger comfort, and adequate control of dynamic tyre loads, thus ensuring vehicle safety and stability. The dynamic tyre load is associated with the reduction in a tyre's ability to generate shear forces if the load on it is fluctuating substantially

about the mean value. A relatively low value of dynamic tyre load implies relatively little impairment of shear force generation and hence good vehicle manoeuvrability due to road roughness (Sharp and Hassan 1986). This must be designed within a finite amount of space, which acts as a constraint to the designer. The three main criteria often used to assess vehicle performance are therefore:

- RMS car body acceleration,

- RMS dynamic wheel contact force,

- RMS suspension working space.

It transpires that these fundamental features of suspension design are effectively captured in the quarter car model (Crolla 1996) which has therefore been used in this study. Figure 12(a) shows a schematic quarter car model with an idealised passive suspension. Parameters were chosen so as to represent a typical family saloon car and are shown in Table 2. To characterise performance, the above three performance indicators were calculated, where lower values correspond to superior performance levels.

5.2   Quarter car configurations

Five configurations of suspension damper were investigated and these configurations are described below.

- **Passive**

As for the SDOF study, the passive quarter car model (shown in Figure 12(a)) was investigated to provide a useful performance benchmark to assess the MR systems. The damping coefficient C_p was varied between 1kNs/m and 5kNs/m, which approximately corresponds to sprung mass damping ratios between 0.2 and 1.

- **MR linearised modified skyhook control**

For 2DOF systems such as the quarter car, skyhook control attenuates vibration at the natural frequency of the sprung mass but has an adverse effect at the natural frequency of the wheel mass (wheel hop frequency). This has led to an alternative strategy known as modified skyhook control which combines the concept of skyhook damping with passive damping as an attempt to gain the advantages of both (Cebon *et al.* 1996). With reference to Figure 12(b) and Figure 4(a), the set-point control force F_d is given by:

$$F_d = D_{MRm}(\alpha(\dot{x}_c - \dot{x}_w) + (1 - \alpha)\dot{x}_c) \tag{8}$$

Here, α is a weighting parameter between 0-1. $\alpha = 1$ corresponds to a viscous set-point damping force thus emulating the passive system and $\alpha = 0$ corresponds to a pure skyhook set-point force. As before, the desired force will only be achieved accurately if it is within the control limits of the MR damper (see Figure 5).

- **On/off modified skyhook control**

The input current for the on/off controller is given by:

$$I = I_{max}: \qquad (\alpha(\dot{x}_c - \dot{x}_w) + (1 - \alpha)\dot{x}_c)(\dot{x}_c - \dot{x}_w) \geq 0 \text{ - Energy dissipation required} \tag{9}$$

$$I = 0: \qquad (\alpha(\dot{x}_c - \dot{x}_w) + (1 - \alpha)\dot{x}_c)(\dot{x}_c - \dot{x}_w) < 0 \text{ - Energy input required} \tag{10}$$

- **Fully active modified skyhook control**

With reference to Figure 12(c), the ideal damping force F is given by:

$$F = D_{ISm}(\alpha(\dot{x}_c - \dot{x}_w) + (1 - \alpha)\dot{x}_c) \tag{11}$$

- **Ideal semi-active modified skyhook control**

Again referring to Figure 12(c), the ideal semi-active damping force is given by:

$$F = D_{SASm}(\alpha(\dot{x}_c - \dot{x}_w) + (1-\alpha)\dot{x}_c): \qquad \dot{x}_c(\dot{x}_c - \dot{x}_w) \geq 0 \qquad (12)$$

$$F = 0: \qquad \dot{x}_c(\dot{x}_c - \dot{x}_w) < 0 \qquad (13)$$

5.3 Real road disturbance

In order to realistically assess the capability of the MR damper as part of a vehicle suspension, a broadband random signal, representative of a typical road was generated to provide an input to the quarter car model. The profile of a single track along the length of a road surface can be approximately described by a displacement power spectral density function (PSD) $S(n)$ at wavenumber n (cycles/m), as follows (Robson 1979):

$$S(n) = Cn^{-w} \qquad \left(\frac{m^2}{cycle/m}\right) \qquad (14)$$

Here, C and w are fitting constants describing the severity of road roughness. The wavenumber n is given by f/V, where f is the vibration frequency and V is the vehicle speed. Consequently, for a given vehicle speed, the inverse fast Fourier transform can be used to determine the road surface heights in the time domain (Cebon and Newland 1984). Motorway, principal and minor road excitations were generated with frequency content between 0-15Hz. Table 3 shows the corresponding values of C, w and V and Figure 13 shows a typical motorway excitation in the time and frequency domain.

5.4 Results

To begin, Figure 14(a) shows the PSD of wheel contact force for the MR linearised modified skyhook system. The responses shown are for the motorway excitation and are compared to the passive system with $C_p = 2$kNs/m, which corresponds to a damping ratio of 0.4. For the MR system, responses are shown for a range of α with controller gain $D_{MRm} = 3$kNs/m. In the pure skyhook case ($\alpha = 0$), the vibration at the sprung mass natural frequency has been

significantly reduced but, as expected, an adverse effect at the wheel hop frequency is observed. It can be seen how increasing α, and thus augmenting the system with passive damping, improves this by allowing the magnitudes of the two resonant peaks to be compromised against one another. Through appropriate parameter selection, the MR system is clearly superior to the passive system.

Similarly, Figures 14(b) and 14(c) compare the motorway PSD plots of the passive system with the fully active and ideal semi-active modified skyhook systems respectively. Skyhook gains equal to 3kNs/m have been used in both cases. A key difference between the fully active/ideal semi-active systems and the MR linearised system is in the mid frequency range (3-9Hz), where the fully active/ideal semi-active systems achieve much lower vibration levels. Reducing the damping rate at 0A, for example by changing vehicle parameters or fluid properties, should improve the MR system in this range and push the performance levels nearer to the ideal semi-active system. It can also be observed how the performance levels of fully active and ideal semi-active systems are similar for values of α which give acceptable levels of wheel hop vibration.

Next, the on/off modified skyhook system is investigated. Figure 14(d) shows the PSD of wheel contact force for the controller gain $I_{max} = 0.06$A. Again, the motorway excitation has been used as an example. The vibration at the sprung mass natural frequency is clearly lower than the passive system, however the wheel hop response is very poor with no significant gain in performance when α is increased. A pure skyhook strategy ($\alpha = 0$) is therefore optimal for the on/off control strategy.

As with the SDOF system, the conflict diagram can be used to optimise and compare each control strategy. For the quarter car model, these have been constructed by plotting RMS car

body acceleration and RMS wheel contact force versus the RMS suspension working space for each road excitation. Figure 15 shows the resulting conflict curve comparing each vehicle configuration subject to the motorway excitation. Each modified skyhook system has already been optimised in terms of the controller gain (D_{MRm} = 3kNs/m, D_{ISm} = 3kNs/m and D_{SASm} = 3kNs/m) where that value which best minimised car body acceleration was chosen. With the exception of on/off control (where it has already been established that skyhook control is optimal), each curve shown corresponds to the range α = 0-1. The on/off conflict curve corresponds to a range of controller gains I_{max} for α = 0 and the passive response corresponds to the range C_p = 1-5kNs/m.

As observed in the SDOF study, the MR linearised modified skyhook system can be observed to outperform the on/off controller. Nonetheless, the on/off controller does perform well, outperforming the passive system.   The superiority of the linearised system is more obvious in terms of wheel contact force because, unlike the on/off controller, MR linearised modified skyhook control is able to suppress the wheel hop vibrations. However, RMS wheel contact force for the linearised system is still on a par with the passive system. This is partly due to the way in which the controller gains were optimised in terms of car body acceleration as outlined previously. It is well known that ride comfort will be traded off against vehicle handling and optimising the controller gain in terms of wheel contact force should improve this result.

To investigate the effect of the operating conditions on performance, a specific operating point (α or I_{max}) has been chosen and maintained for the three excitation conditions (motorway, principal and minor road). The performance of each controlled system has then been rated as a percentage improvement over the passive system with C_p=2kNs/m (which corresponds to a damping ratio of 0.4). The operating points were chosen, using the

motorway conflict diagram (Figure 15), so as to minimise car body acceleration whilst maintaining adequate wheel contact force and suspension working space levels that are similar to the passive system. The corresponding operating points are indicated on Figure 15 and are tabulated in Table 4, and Figure 16 shows the results in graphical form. By first taking the motorway excitation as an example, the linearised system demonstrates a 10% improvement in RMS acceleration whilst maintaining similar wheel contact force levels to the passive system, whereas the on/off system results in a 3% reduction in RMS acceleration but RMS wheel contact force is 4% worse than the passive system. There is a 9% and 13% improvement in RMS suspension working space for the linearised and on/off system respectively. By analysing the full excitation range, the results re-iterate the key advantage in using feedback linearisation, which was demonstrated for the SDOF system. From Figure 16, it can be observed how the MR linearised operating point is insensitive to changes in the input conditions. This is seen through the steady performance levels, which are consistently superior to the passive system across the full excitation range. Furthermore, the car body acceleration is similar to the fully active and ideal semi-active systems. In contrast to the linearised system, the optimum controller gain for the on/off controller is highly dependant on the input conditions. This is seen through the progressive deterioration of suspension working space as the harshness of the road surface worsens.

For some performance criteria, the MR systems can be observed to outperform the fully active and ideal semi-active systems. For example, the RMS suspension working space of the on/off system is superior for the motorway excitation (Figure 16(a)), and the car body acceleration of the linearised system is slightly superior for the principal road excitation (Figure 16(b)). However the fully active/ideal semi-active systems always outperform the MR systems in two out of the three performance indicators.

20

6 DISCUSSION

Using skyhook derived control laws, this paper has demonstrated for both SDOF and 2DOF systems, how feedback linearisation can better harness the controllability of a smart fluid damper when compared to more straightforward on/off control strategies.

In the SDOF study, the fully active and ideal semi-active systems demonstrate superior acceleration levels when compared to the MR systems but this is at the expense of poorer suspension working space levels. Fully active control is particularly superior if these larger working spaces can be tolerated. However, the 2DOF study did not demonstrate such advantages with the ideal semi-active system closely approaching the fully active system. This suggests that dissipative energy is required for most of the time. Furthermore, the similarity between the MR and ideal semi-active system suggests that the MR performance could be further enhanced by designing the system with a lower 'off-state' damping rate.

A key advantage of feedback linearisation is how the damping behaviour becomes less sensitive to external changes. For example, environmental effects and manufacturing tolerances, which would result in varying fluid properties, should have no major effect on performance. On the other hand, it is probable that degradation in the performance of an on/off system, and a shift in the controller gain would be observed when such effects play a role. When this effect is coupled with the changing optimum controller gain due to changes in the input conditions, performance could seriously suffer. This needs to be experimentally validated and will be an interesting focus for future work.

Step response tests might also provide an interesting focus for further work. It is possible that on/off control strategies may outperform continuous feedback strategies in this scenario since the onset of maximum damping will occur sooner. Step tests have been omitted from the

21

present study as the MR damper model is yet to be validated for the high velocity inputs that would be induced.

7 CONCLUSIONS

This article has investigated the feedback control of vibration isolation systems using smart fluid dampers. The vibrating systems were investigated using broadband mechanical excitations, and the results have been benchmarked against ideal passive, semi-active, and fully active systems.

Two control strategies have been studied: feedback linearisation, and on/off control. New experimental results have demonstrated that feedback linearisation is effective under broadband mechanical excitation, and that the proposed model remains valid under these conditions.

A single-degree-of-freedom mass-isolator problem has been investigated numerically, and MR linearised skyhook control was shown to be superior to on/off skyhook control, demonstrating a 25% reduction in acceleration over an optimised passive system compared to 15% for the on/off strategy. The ideal semi-active and fully active systems outperformed both of the MR damper systems in terms of acceleration, but this was at the expense of larger working spaces.

A two-degree-of-freedom system representing a vehicle quarter car model was then investigated numerically. The MR linearised controller, in conjunction with a modified skyhook strategy, was able to outperform the passive system by 10% in terms of car body acceleration and suspension working space, without affecting the wheel contact forces. In contrast, the on/off control strategy was unable to significantly improve the car body acceleration and the suspension working space simultaneously. The fully active and ideal

semi-active systems were generally superior to the MR systems, where performance was better in at least two of the three performance indicators investigated. Nonetheless, car body acceleration levels for the MR linearised system were comparable to the fully active/ideal semi-active systems.

For both of the isolation systems, the feedback linearisation strategy was shown to be relatively insensitive to changes in the input excitation conditions. On the other hand, the on/off strategy was highly sensitive to the input excitation.

Finally, further work will be required to compare the numerical results with experimental predictions, and to compare alternative smart fluid damper control strategies (e.g. sliding mode control) in a similar fashion.

ACKNOWLEDGEMENTS

REFERENCES

Atray, V.S. and Roschke, P.N. (2004). "Neuro-fuzzy control of railcar vibrations using semiactive dampers." *Computer-Aided Civil and Infrastructure Engineering*, **19**(2), 81-92.

Cebon, D. and Newland, D.E. (1984). "The artifical generation of road surface topography by the inverse FFT method", *Proceedings of the 8th IAVSD symposium on the dynamics of vehicles on roads and railway tracks*, Cambridge, Massachussets, Swets and Zeitlinger, 29-42.

Cebon, D., Besinger, F.H. and Cole, D.J. (1996). "Control strategies for semi-active lorry suspensions." *Proceedings of the Institution of Mechanical Engineers, Part D: Journal of automobile engineering*, **210**, 161-178.

Choi, Y.T. and Wereley, N.M. (2003). "Vibration control of a landing gear system featuring electrorheological/magnetorheological fluids." *Journal of Aircraft*, **40**(3), 432-439.

Crolla, D.A. (1996). "Vehicle dynamics: theory into practice." *Proceedings of the Institution of Mechanical Engineers, Part D: Journal of automobile engineering*, **210**, 83-94.

Dyke, S.J., Spencer, B.F.J., Sain, M.K. and Carlson, J.D. (1998). "Experimental study of MR dampers for seismic protection." *Smart Materials and Structures*, **7**(5), 693-703.

Guo, D.L., Hu, H.Y. and Yi, J.Q. (2004). "Neural Network Control for a Semi-Active Vehicle Suspension with a Magnetorheological Damper." *JVC/Journal of Vibration and Control*, **10**(3), 461-471.

Jansen, L.M. and Dyke, S.J. (2000). "Semiactive control strategies for MR dampers: Comparative study." *Journal of Engineering Mechanics*, **126**(8), 795-803.

Jolly, M., Bender, J.W. and Carlson, J.D. (1998). "Properties and applications of commercial magnetorheological fluids." *SPIE 5th international symposium on Smart Structures and Materials, San Diego*, **3327**, 262-275.

Karnopp, D., Crosby, M.J. and Harwood, R.A. (1974). "Vibration control using semi-active force generators." *Journal of Engineering for Industry*, **96**, 619-626.

Lam, A.H.F. and Liao, W.H. (2003). "Semi-active control of automotive suspension systems with magneto-rheological dampers." *International Journal of Vehicle Design*, **33**(1-3), 50-75.

Lord Corporation (2004), http://www.lord.com/Default.aspx?tabid=761.

Robson, J.D. (1979). "Road surface description and vehicle response." *International Journal of Vehicle Design*, **1**(1), 25-35.

Sharp, R.S. and Hassan, S.A. (1986). "The relative performance capabilities of passive, active and semi-active car suspension systems." *Proceedings of the Institution of Mechanical Engineers, Part D: Journal of automobile engineering*, **200**, 219-228.

Simon, D. and Ahmadian, M. (2001). "Vehicle evaluation of the performance of magnetorheological dampers for heavy truck suspensions." *Journal of Vibration and Acoustics*, **123**, 365-375.

Sims, N.D., Stanway, R. and Johnson, A.R. (1999a). "Vibration control using smart fluids: A state of the art review." *The shock and vibration digest*, **31**(3), 195-203.

Sims, N.D., Peel, D.J., Stanway, R., Johnson, A.R. and Bullough, W.A. (1999b). "The electrorheological long stroke damper: A new modelling technique with experimental validation." *Journal of Sound and Vibration*, 207-227.

Sims, N.D., Peel, D.J., Stanway, R., Bullough, W.A. and Johnson, A.R. (1999c). "Controllable viscous damping: An experimental study of an electrorheological long stroke damper under proportional feedback control." *Smart Materials and Structures*, **8**, 601-605.

Sims, N.D., Stanway, R., Peel, D.J., Bullough, W.A. and Johnson, A.R. (2000). "Smart fluid damping: Shaping the force/velocity response through feedback control." *Journal of Intelligent Material Systems and Structures*, **11**, 945-949.

Sims, N.D., Stanway, R. and Johnson, A.R. (2001). "Experimental testing and control of an ER long-stroke vibration damper." *Smart Structures and Materials: Smart Systems for Bridges, Structures and Highways, Proceedings of SPIE*, **4330**, 218-227.

Sims, N.D. and Stanway, R. (2003). "Semi-active vehicle suspension using smart fluid dampers: A modelling and control study." *International Journal of Vehicle Design*, **33**(1-3), 76-102.

Sims, N.D. and Wereley, N.M. (2003). "Modelling of Smart fluid dampers." *Smart Structures and Materials: Passive damping and isolation, SPIE*, **5052**, 163-175.

Sims, N.D., Holmes, N.J. and Stanway, R. (2004). "A unified modelling and model updating procedure for electrorheological and magnetorheological dampers." *Smart Materials and Structures*, **13**, 100-121.

Welch, P.D. (1967). "The use of fast fourier transform for the estimation of power spectra: A method based on time averaging over short, modified periodograms." *IEEE Trans. Audio Electroacoust*, **AU-15**, 70-73.

xPC Target (2002). The MathWorks, Inc., 3 Apple Hill Drive, Natick, MA.

Xu, Z.D., Shen, Y.P. and Guo, Y.Q. (2003). "Semi-active control of structures incorporated with magnetorheological dampers using neural networks." *Smart Materials and Structures*, **12**(1), 80-87.

Yi, F., Dyke, S.J., Caicedo, J.M. and Carlson, J.D. (2001). "Experimental verification of multiinput seismic control strategies for smart dampers." *Journal of Engineering Mechanics*, **127**(11), 1152-1164.

Yoshida, O. and Dyke, S.J. (2004). "Seismic control of a nonlinear benchmark building using smart dampers." *Journal of Engineering Mechanics*, **130**(4), 386-392.

Control strategy	Controller gain
Passive	C_p = 3kNs/m
MR linearised skyhook	D_{MR} = 4kNs/m
On/off skyhook	I_{max} = 0.5A
Fully active skyhook	D_{IS} = 7kNs/m
Ideal semi-active skyhook	D_{SAS} = 6kNs/m

Table 1: Controller parameters for the optimised mass-isolator systems.

Mass of car body	M_c (kg)	300
Mass of wheel assembly	M_w (kg)	35
Suspension stiffness	K (N/m)	20000
Tyre stiffness	K_w (N/m)	200000
Passive damping rate	C_p (Ns/m)	1000-5000
Tyre damping rate	C_w (Ns/m)	80

Table 2: Quarter car suspension parameters.

Profile	C	w	V (miles/hr)
Motorway	7×10^{-8}	2.5	70
Principal road	50×10^{-8}	2.5	60
Minor road	500×10^{-8}	2.5	30

Table 3: Road profile parameters.

Control strategy	Controller gain	α
Passive	C_p = 2kNs/m	-
MR linearised modified skyhook	D_{MRm} = 3kNs/m	0.25
On/off skyhook	I_{max} = 0.08A	0
Fully active modified skyhook	D_{ISm} = 3kNs/m	0.6
Ideal semi-active modified skyhook	D_{SASm} = 3kNs/m	0.6

Table 4: Controller parameters for the optimised vehicle suspension systems.
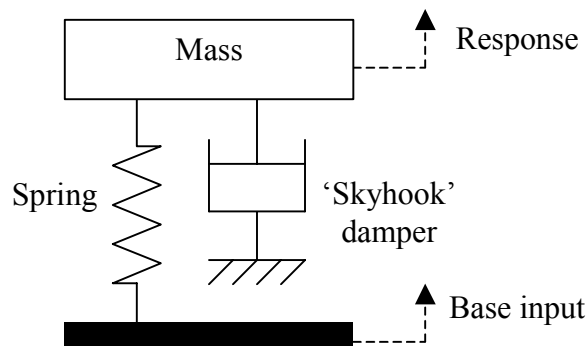
Figure 1: Skyhook control of an SDOF mass-isolator.

(a)

(b)
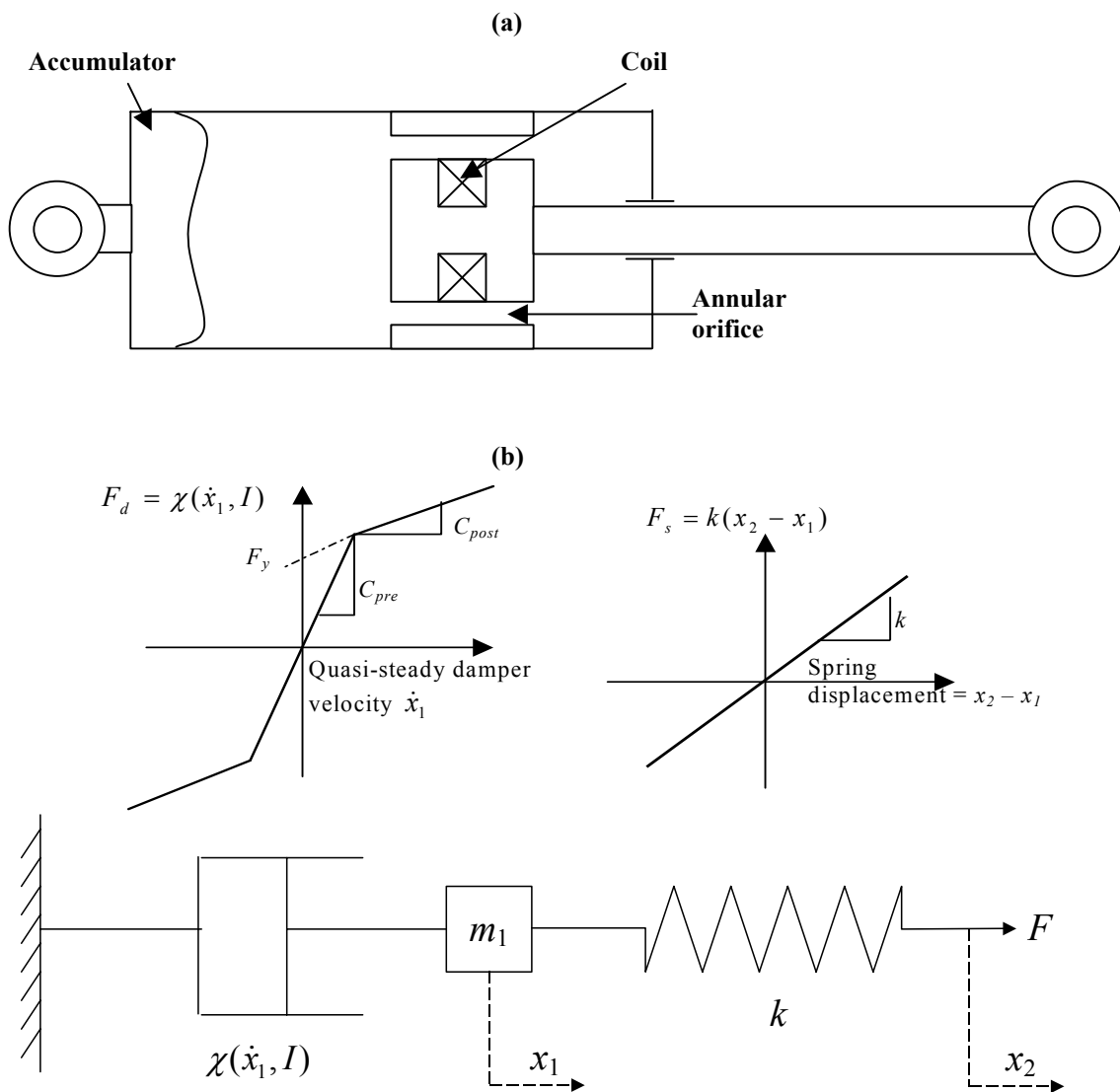
Figure 2: (a) Schematic diagram of the MR damper and (b) the lumped parameter model.

(a)   **(b)**
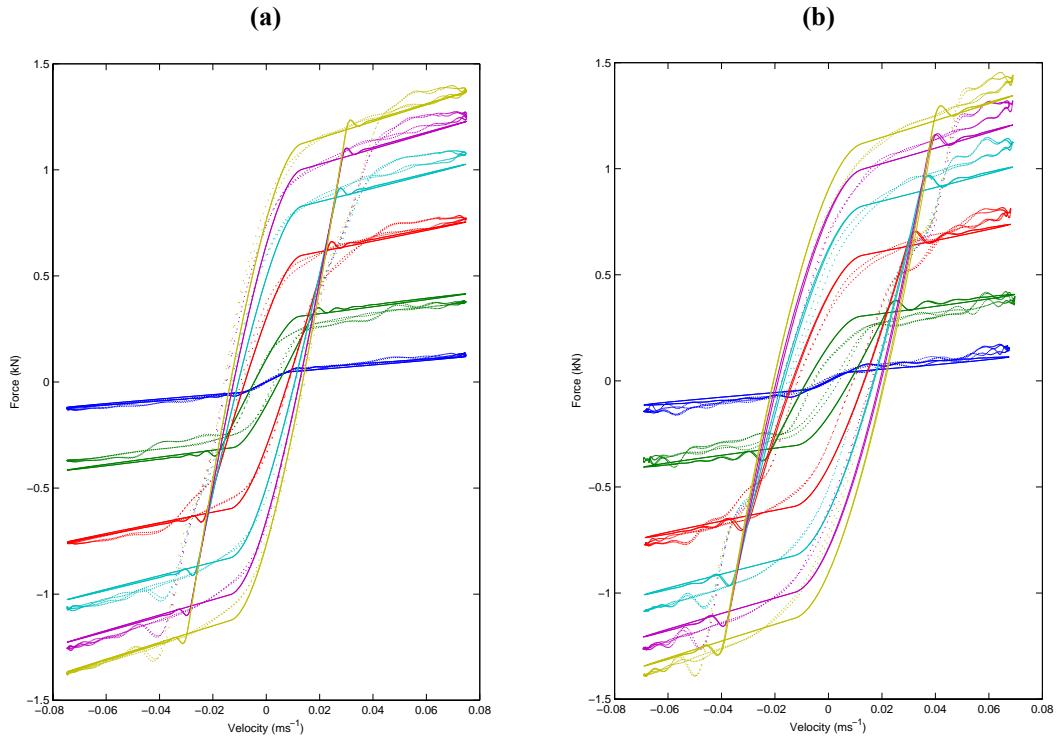
Figure 3: Simulated and experimental MR damper response. 0, 0.2, …, 1.0A (Sims *et al.* 2004).
• **Experimental —— Simulated**
(a) 6Hz, 2mm (b) 12 Hz, 1mm

(a)

(b)
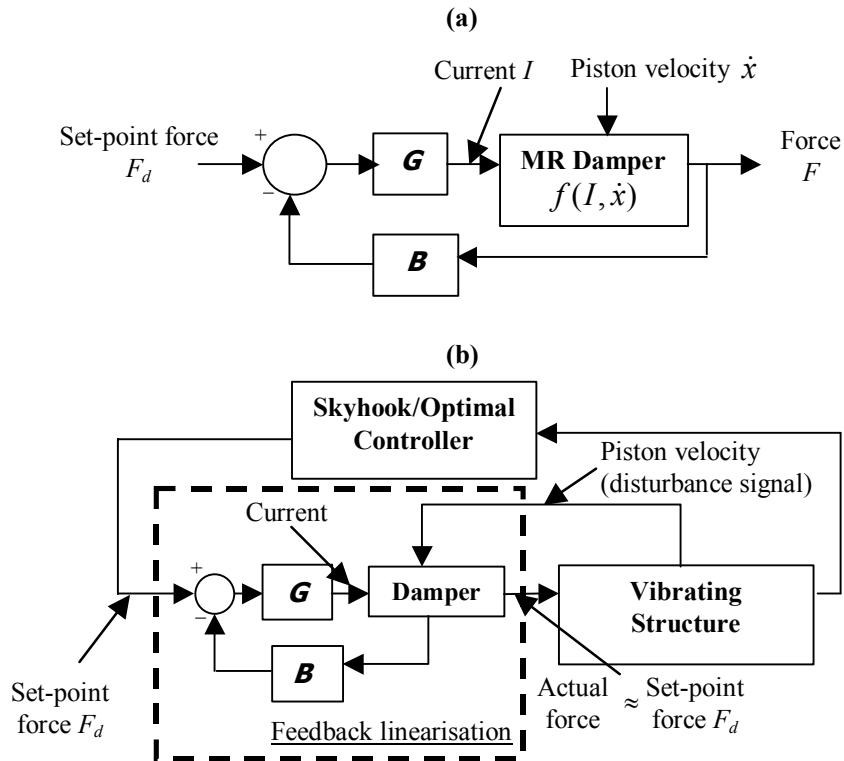
Figure 4: Semi-active force generator. (a) Controller block diagram and (b) implementation within a controlled vibration system.
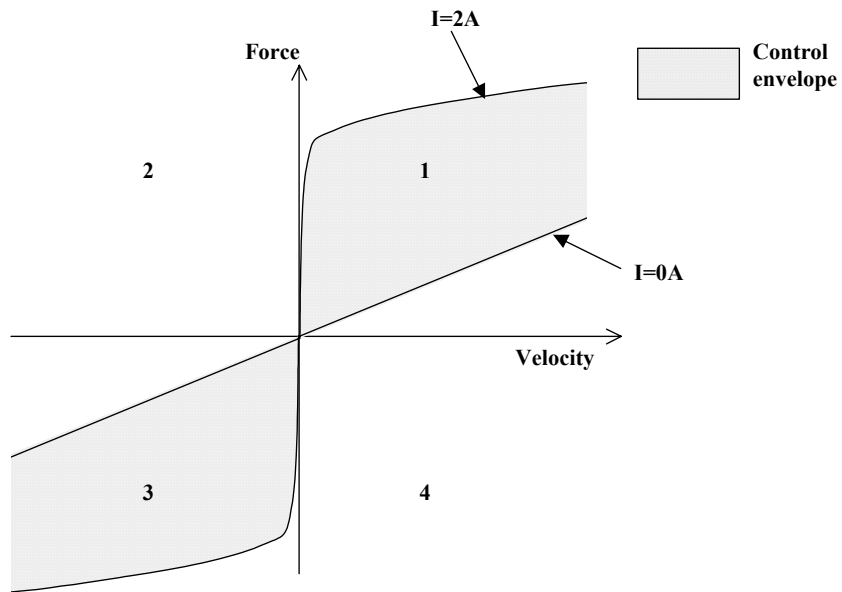
Figure 5: Control envelope of the MR damper.
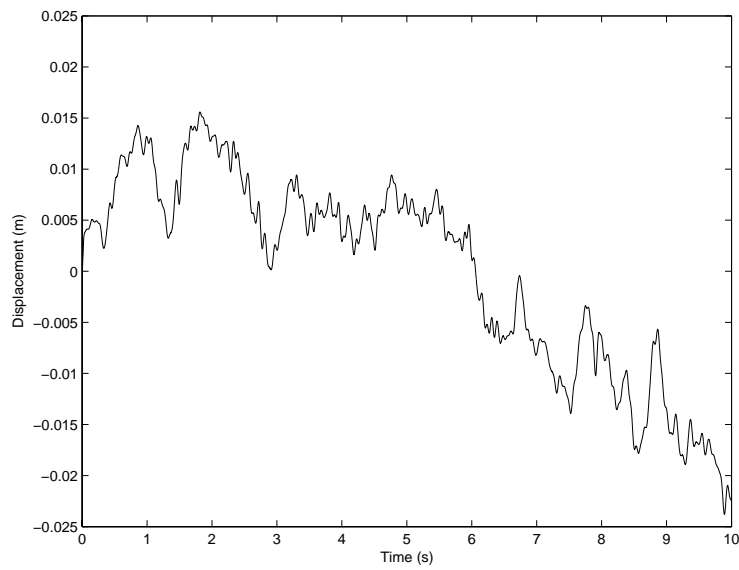
Figure 6: Broadband input excitation used for experimental validation of feedback linearisation.
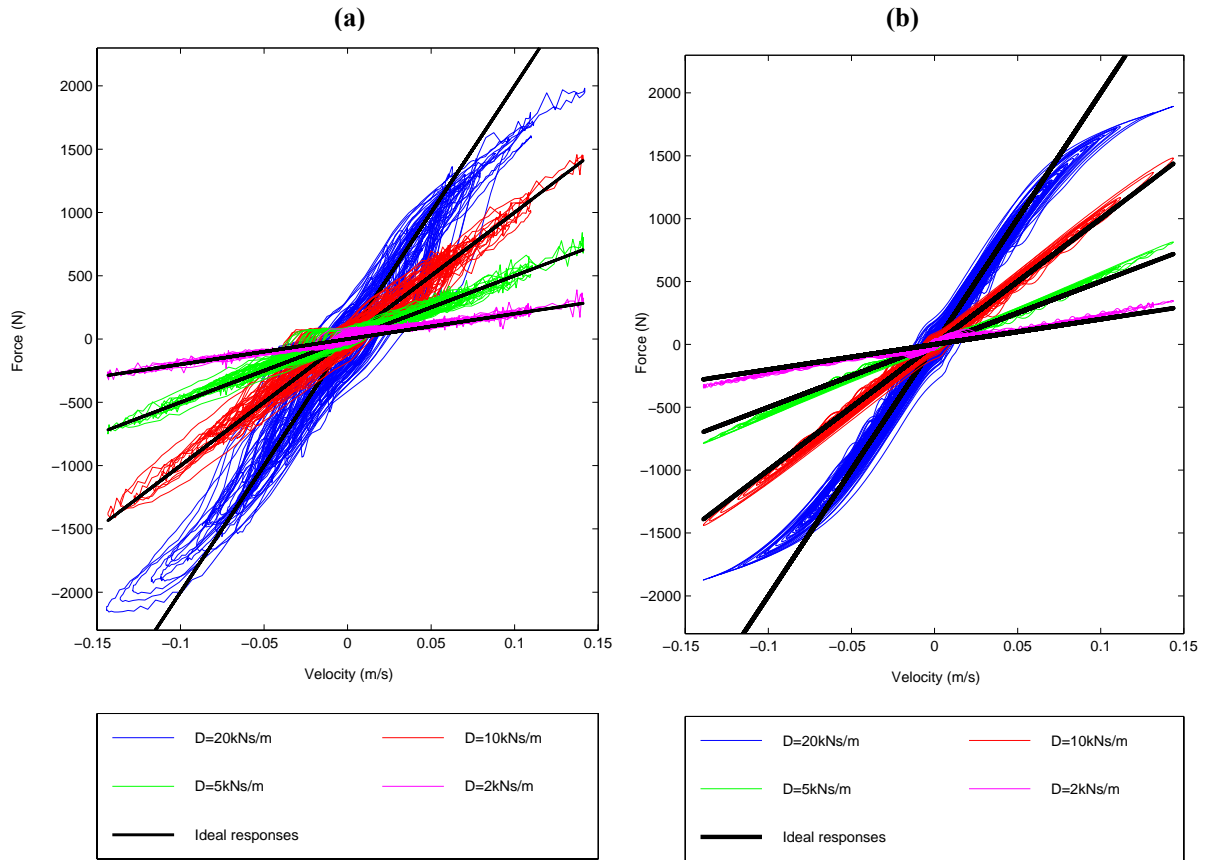
Figure 7: Linearised force-velocity responses, G=0.0015, B=0.6. (a) Experimental and (b) simulated.
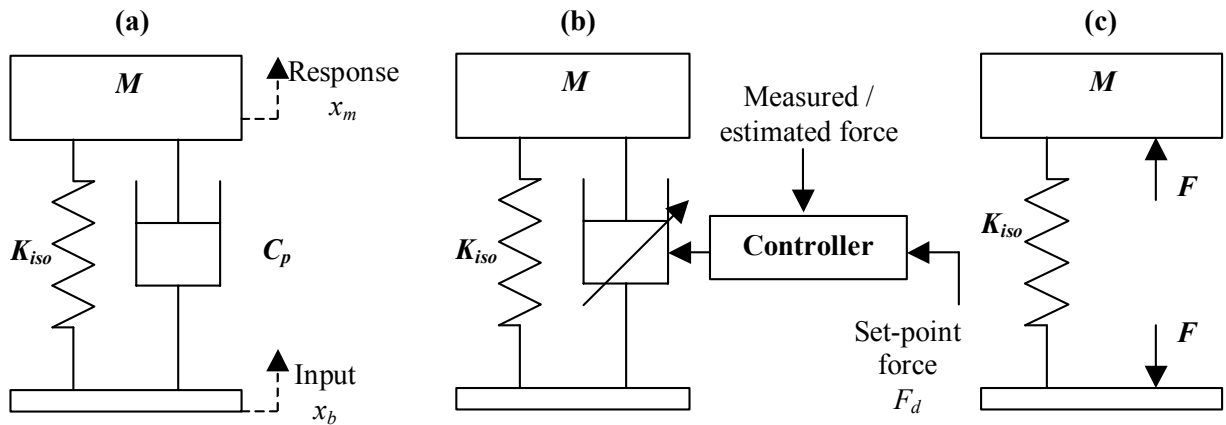
Figure 8: Mass-isolator models. (a) Passive system, (b) MR linearised system and (c) ideal system.
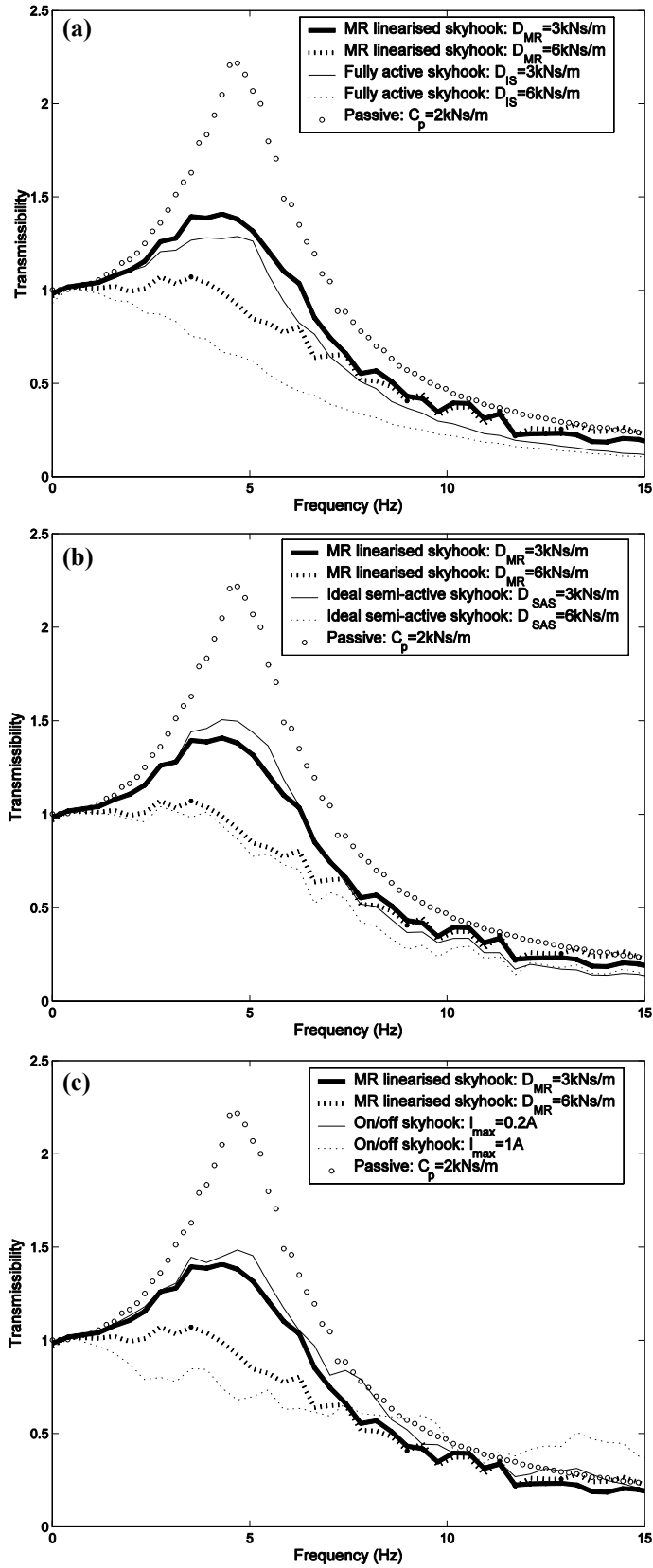
Figure 9: Transmissibility comparisons between (a) linearised MR skyhook and fully active skyhook systems, (b) linearised MR skyhook and idealised semi-active skyhook systems and (c) linearised MR skyhook and on/off MR skyhook systems. Input signal with cut-off frequency at 25Hz.
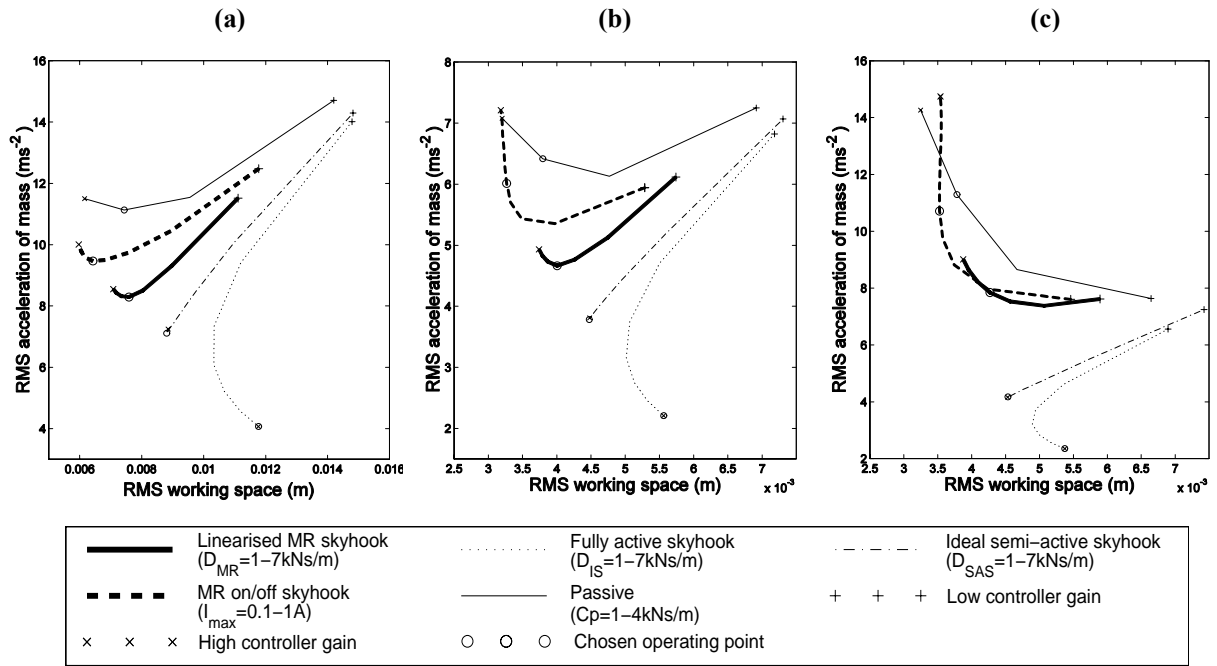
Figure 10: Conflict curves for each mass-isolator configuration. (a) Input displacement filtered to 10Hz, (b) input displacement filtered to 25Hz and (c) unfiltered input with frequency components up to 100Hz.
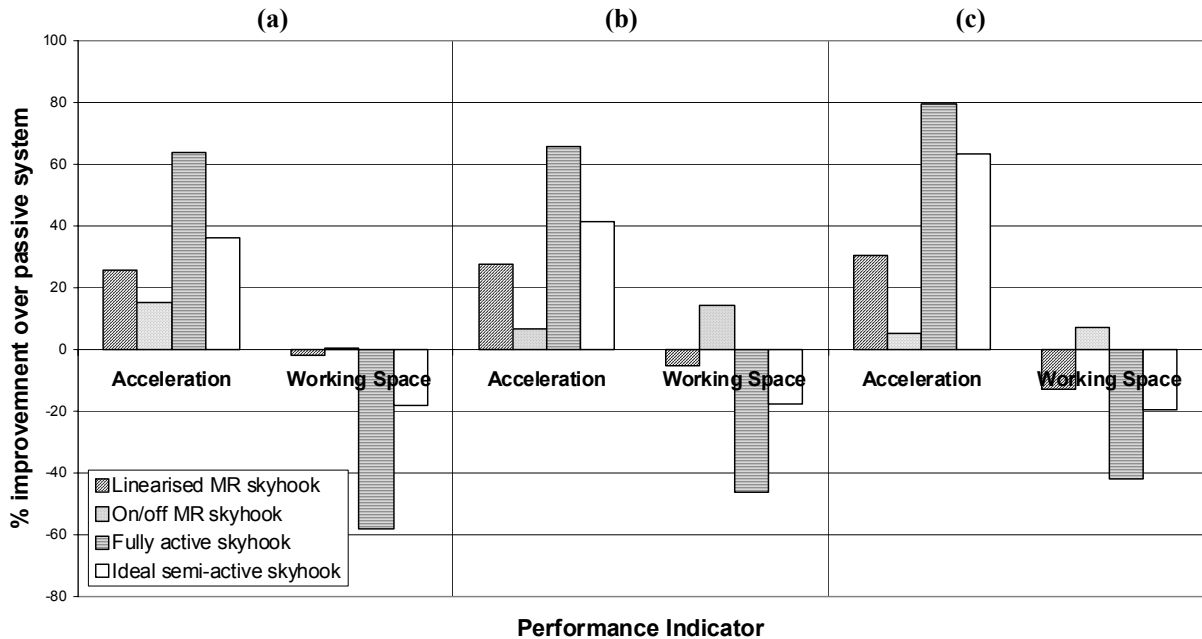
Figure 11: The % performance improvements of the MR and idealised systems over the passive system. (a) Input displacement filtered to 10Hz, (b) input displacement filtered to 25Hz and (c) unfiltered input with frequency components up to 100Hz. Controller parameters correspond to those given in Table 1.
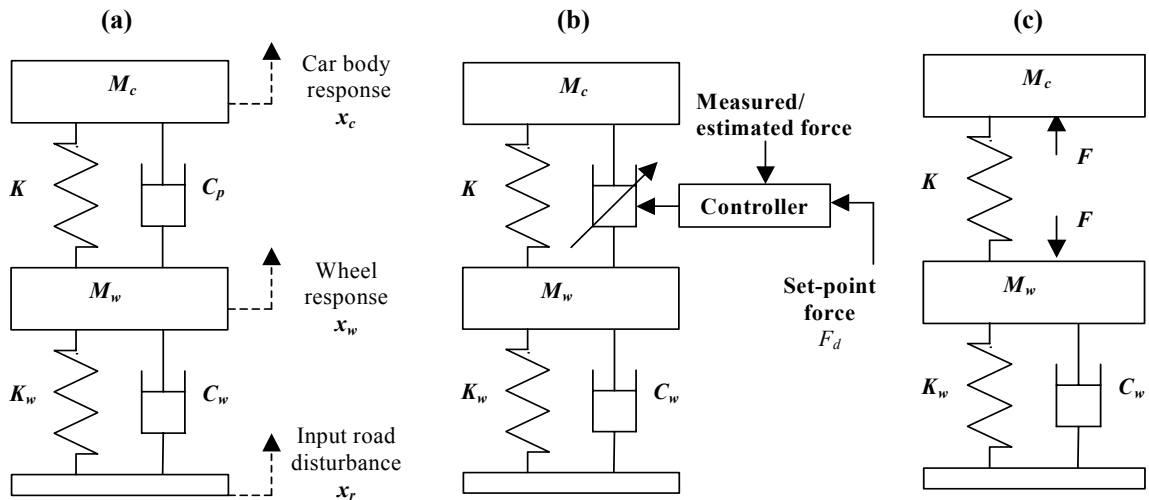
Figure 12: Quarter car models. (a) Passive system, (b) MR linearised system and (c) ideal system.
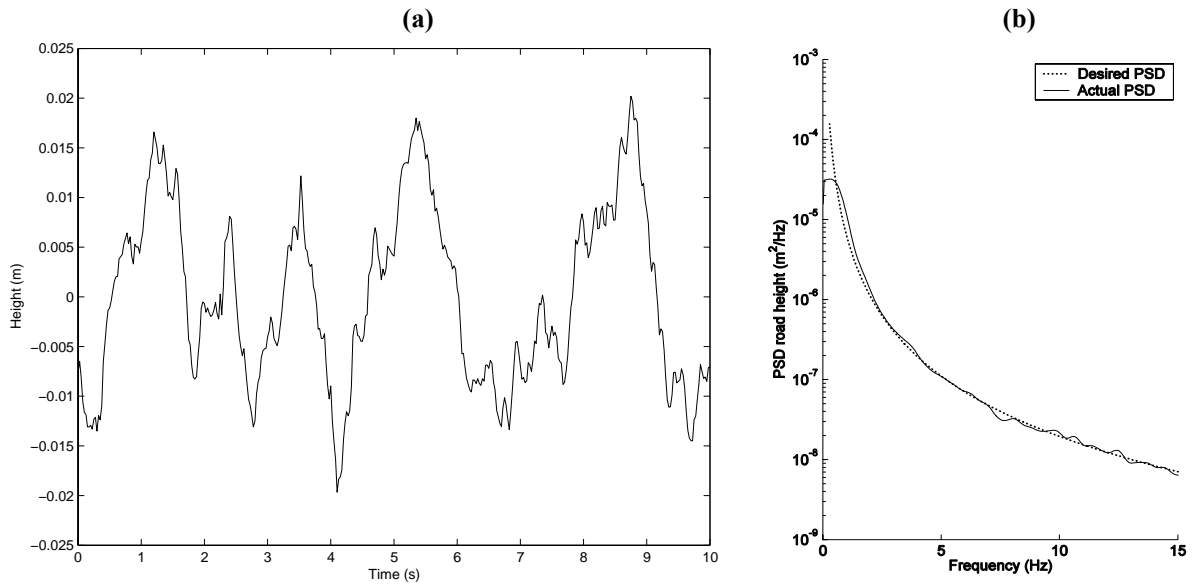
Figure 13: Motorway excitation. (a) Time history and (b) a comparison between the desired and actual power spectral density.
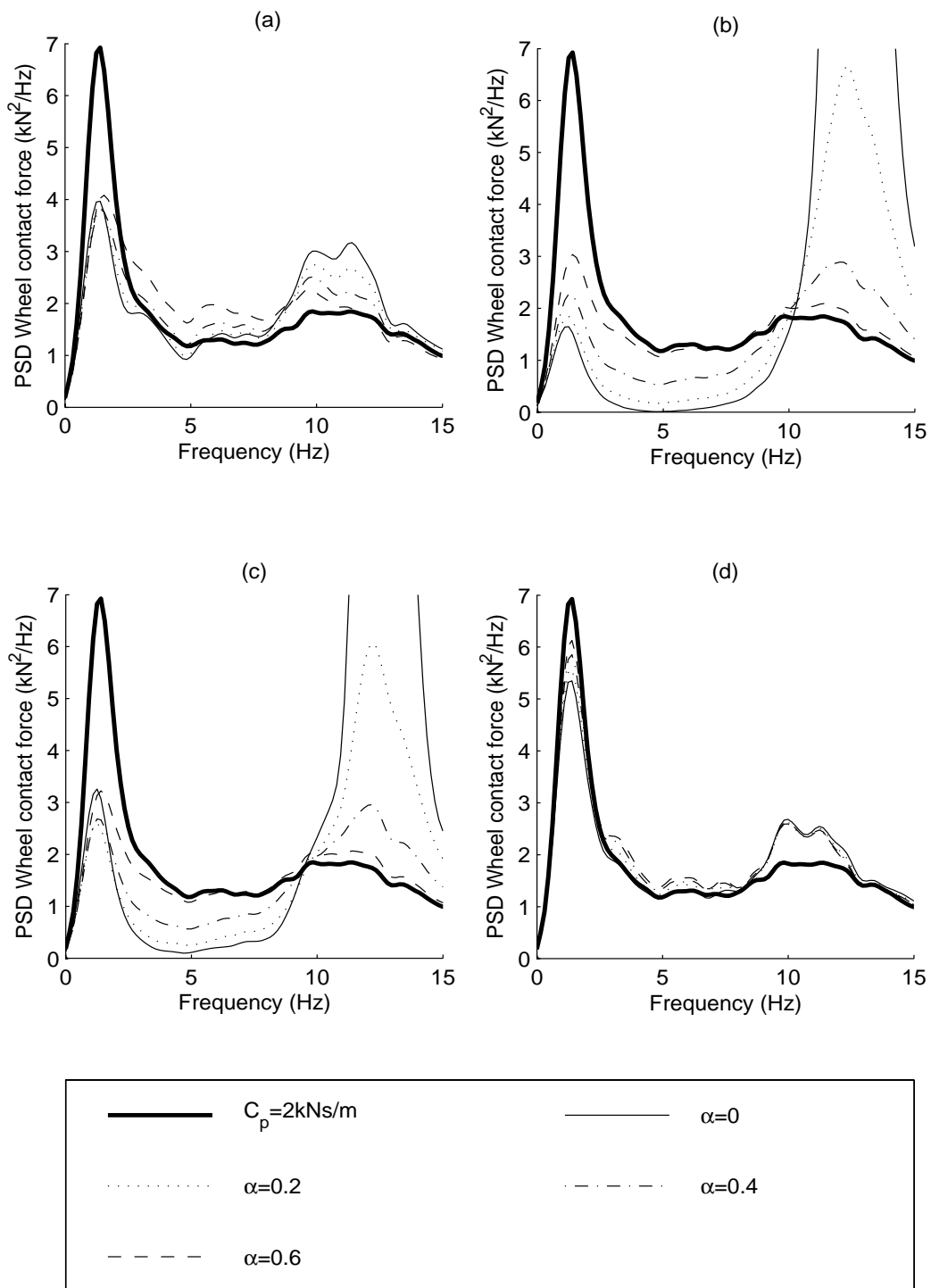
Figure 14: Frequency response to the motorway excitation. (a) MR linearised modified skyhook system - D_{MRm} = 3kNs/m, (b) fully active modified skyhook system - D_{ISm} = 3kNs/m, (c) ideal semi-active modified skyhook system - D_{SASm} = 3kNs/m and (d) MR on/off modified skyhook system -I_{max} = 0.06A.
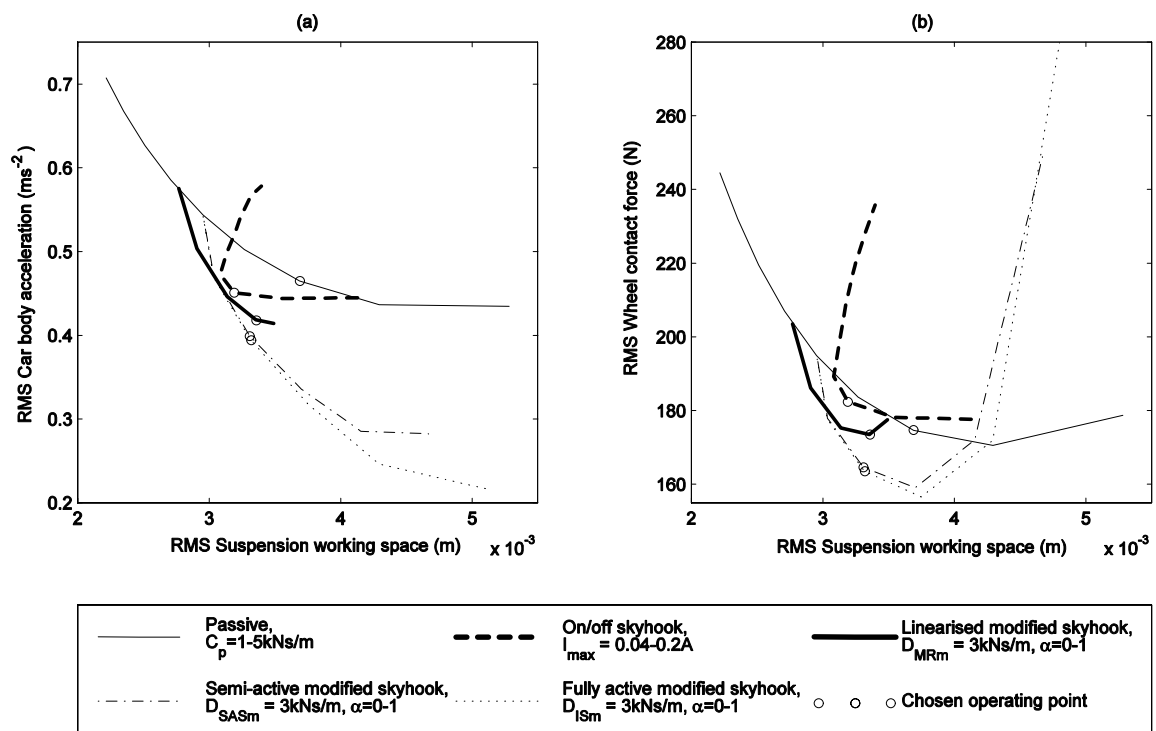
Figure 15: Conflict diagrams comparing each vehicle control strategy. Motorway excitation.
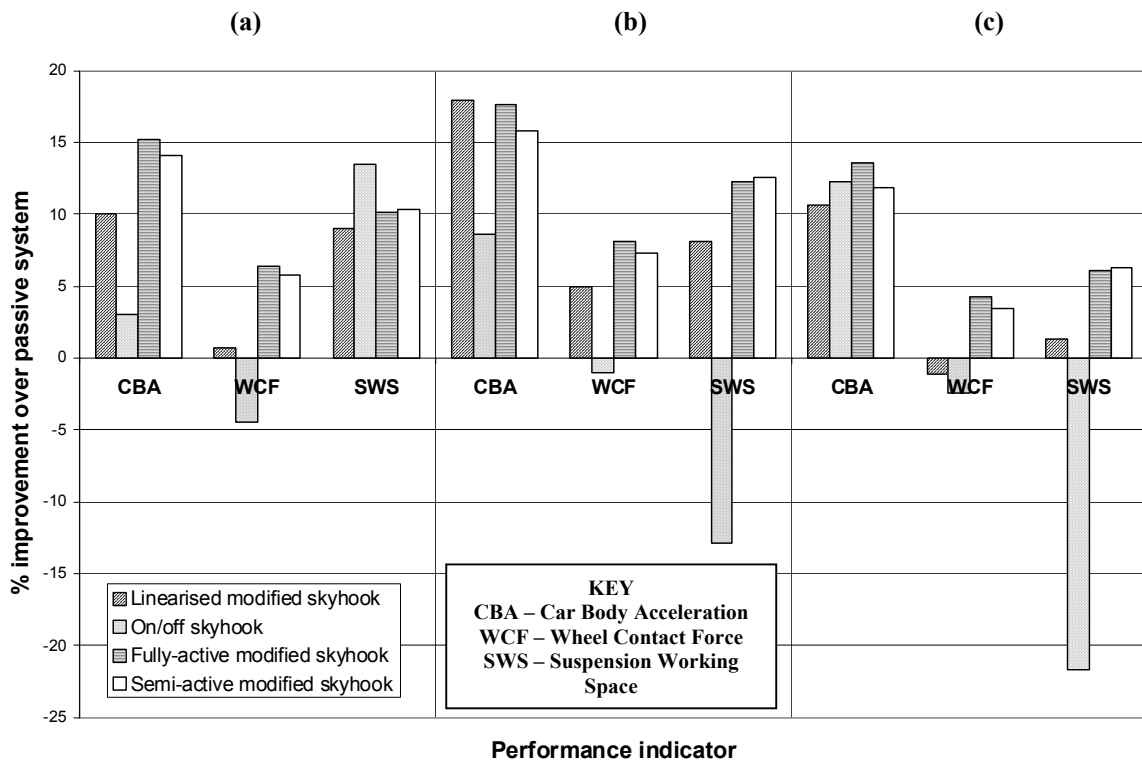
Figure 16: The % performance improvements of the MR and idealised systems over the passive system. (a) Motorway excitation, (b) principal road excitation and (c) minor road excitation. Controller parameters correspond to those given in Table 4.

KEYWORDS

Smart fluids; magnetorheological damper; semi-active control; benchmarking; mass isolator; vehicle suspension; skyhook; feedback linearisation.

TABLE LIST

FIGURE LIST

36